A fully humanized von Willebrand disease type 1 mouse model as unique platform to investigate novel therapeutic options

Geneviève McCluskey,[1*] Marco Heestermans,[1*] Ivan Peyron,[1] Eloise Pascal,[2] Marie Clavel,[2] Eric Bun,[1] Emilie Bocquet,[1] Christelle Reperant,[1] Sophie Susen,[3] Olivier D. Christophe,[1] Cécile V. Denis,[1] Peter J. Lenting[1#] and Caterina Casari[1#]

[1]Université Paris-Saclay, INSERM, Hémostase Inflammation Thrombose HITh U1176, 94276, Le Kremlin-Bicêtre; [2]Inovarion, Paris and [3]Université de Lille, Inserm, CHU Lille, Institut Pasteur de Lille, U1011-EGID, F-59000 Lille, France

**GMC and MH contributed equally as first authors.*
#PJL and CC contributed equally as senior authors.

Correspondence: C. Casari
caterina.casari@inserm.fr

Received: June 13, 2024.
Accepted: November 21, 2024.
Early view: November 28, 2024.

https://doi.org/10.3324/haematol.2024.286076

Supplementary information

"A fully humanized von Willebrand disease type 1 mouse model as unique platform to investigate novel therapeutic options"

McCluskey G., Heestermans M, et al.

Animal and ethic statement

Housing and experiments were done in accordance with French regulations and the experimental guidelines of the European Community. This project (number APAFIS #32699-2021081611421076 v1) was approved by the local ethical committee of Université Paris-Saclay (comité d'éthique en expérimentation animale no. 26). Males and females were used throughout the study (8-14 weeks old). Mice used in this study had a specific pathogen free (SPF) health status and were housed in ventilated, enriched cages with food and beverage *ad libitum*.

Engineering of hVWD1 mice

Transgenic mice expressing human (h)VWF and hGPIbα instead of the corresponding murine proteins were engineered in a pure 129S2 (129S2/SvPasCrl) genetic background expressing fully functional ADAMTS13.[1,2] For this purpose, the generation of knock-in mice for each of the protein of interest (hVWF and hGPIbα) was entirely outsourced to genOway (Lyon, France). To engineer the 129S2Crl-*Vwf*$^{-/-}$-Tg(*VWF)* mice (Figure 1A), the cDNA of h*VWF* followed by a *hGH* (human growth hormone) polyadenylation site, was inserted within the murine *Vwf* gene, in frame with the endogenous ATG. Such transgene insertion resulted in the inactivation of the murine *Vwf* gene and expression of the h*VWF* gene under the control of endogenous regulatory sequences. The common single nucleotide variant c.2365A>G (p.T789A), associated with increased VWF levels,[3–5] was inserted within the *hVWF* cDNA. To engineer the 129S2Crl-*Gp1ba*$^{-/-}$-Tg*(GP1BA)* mice (Figure 1B), the murine coding sequence was replaced by the human cDNA, without additional changes to the regulatory sequences. Homozygous mice for both humanized proteins, referred to as hVWF- and hGP1BA mice, were then crossed to generate homozygous double knock-in mice 129S2Crl-*Vwf*$^{-/-}$-Tg(*VWF),Gp1ba*$^{-/-}$-Tg*(GP1BA),* referred to as hVWD1 mice. Results presented in this study pertain to hVWD1 mice and littermate controls (named 129S2 or control mice throughout the manuscript).

Genotyping was performed using DNA extracted by ear biopsies using a classic NaOH-based protocol and PCR amplification (KAPA2G Fast Genotyping Mix, Kapa Biosystems, Wilmington, MA) with various primer combinations (Table S1). PCR products were separated by electrophoresis on 1.5% agarose gels (Figure 1D).

Murine blood collection and counts

Blood sampling was performed under isoflurane anesthesia (2-2.5%) with air 0.8L/minute via retro-orbital puncture using glass capillary tubes, unless otherwise specified. Blood was collected in 10% vol/vol triNa-citrate (0.138M) for plasma preparation (obtained by centrifugation 1500xg, 20 minutes at room temperature) or in 10% vol/vol EDTA 50 mM for blood counts. Blood counts were determined with an automatic cell counter (Scil Vet ABC Plus, Horiba Medical, France).

VWF assays

VWF antigen levels were measured in mouse plasma with an in-house enzyme-linked immunosorbent assay, essentially as previously described,[6] using a pair of polyclonal rabbit anti-VWF antibodies (Agilent Technologies, Les Ulis, France). A human pooled normal plasma (Cryopep, Montpellier, France) was used as reference and a standard human plasma (Siemens, Erlangen, Germany) was used as inter-assay control. Alternatively, a pool of monoclonal anti-human VWF antibodies previously produced and recognizing only human VWF has been used as coating antibody (5μg/ml).

VWF activity was assessed in an ELISA-based collagen binding test (VWF:CB) and an automated platelet-based assay (VWF:GPIbR). For VWF:CB, VWF binding to fibrillar, human placental type III collagen (SouthernBiotech, Birmingham, USA, 5ug/ml) was detected using a polyclonal rabbit anti-VWF antibody. A human pooled normal plasma was used as reference. Immunoturbidimetric VWF:GPIbR was assessed in a ACL TOP 550 (reagents and analyzer, Werfen, Bedford USA).

VWF multimer profiling was performed essentially as previously described[7] in 1.5 or 2% agarose gels. VWF was detected with an in-house alkaline phosphatase-conjugated polyclonal anti-VWF and colorimetric alkaline phosphatase-substrate kit (Bio-Rad Laboratories, Hercules, CA, USA). Membranes were imaged with a G:BOX Chemi XT16 Image Systems (Syngene, Bangalore, India).

Alternatively, VWF multimers were separated in 1.5% agarose gels and visualized by an in-gel staining technique.[8] Briefly, gels were fixed in 5% acetic acid/50% isopropanol 30 minutes, washed twice in H_20 and stained four hours with primary antibody (polyclonal rabbit anti-VWF 0.28mg/l in TBS/0.05% Tween-20/5% BSA). After overnight washing in TBS/0.05% Tween-20, gels were incubated four hours with secondary antibody (Amersham CyDye 800 goat-anti-rabbit 0.07mg/l in TBS/0.05% Tween-20/5% BSA) and washed overnight (TBS/0.05% Tween-20). After an additional wash in TBS, gels were scanned at 800nm with an infrared image system (Amersham Typhoon NIR Plus, Cytiva).

Multimer profiles were analyzed using the Gel Analyzer tool of ImageJ (version 1.53).

FVIII activity assay

FVIII activity was measured in a chromogenic assay using the Biophen FVIII-assay kit (Hyphen, Neuville-sur-Oise, France) as instructed. A murine pooled plasma from 129S2 (wild-type) mice was used as reference.

Parallel plate flow perfusion

After general anesthesia with ketamine/xylazine (200mg/kg and 20mg/kg, respectively) blood was collected from mice by intra-cardiac puncture in unfractionated heparin (40U/ml) and PPACK (80μM). Anticoagulated blood was diluted in 1.2 volumes of Tyrode's buffer (137 mM NaCl, 2 mM KCl, 0.3 mM NaH_2PO_4, 5 mM dextrose, 5 mM N-2-hydroxyethylpiperazine-N0-2-ethanesulfonic acid, 12 mM $NaHCO_3$, pH 7.3) and labeled with rhodamine 6G (10 μg/mL). Thrombus formation was evaluated using a Maastricht flow chamber connected to a syringe pump (KD Scientific) in a whole-blood perfusion assay on a fibrillar collagen matrix (50μg/ml horse type I collagen, Chrono-Par, Mast Diagnostic, Amiens, France, incubated over night at 4°C) under arterial shear conditions (shear rate of 3000 s^{-1}). Platelet adhesion was measured after 3 min of blood perfusion followed by 2 min of washing with Tyrode's buffer. Every perfusion was performed with blood from a single mouse donor. Immediately after each perfusion, 20 images were randomly acquired using an inverted epifluorescence microscope (Nikon Eclipse TE2000-U) equipped with a PlanFluor 20x/0.50 objective (Nikon). The percentage of surface covered by fluorescent platelets and the mean fluorescent intensity were calculated using ImageJ (1.53k). Single dots in the graph represent individual mice (average value of 20 images).

KB-V13A12 production and administration

Single domain antibodies (SdAbs) against VWF were generated as described[9] by screening of a proprietary immune sdAb library obtained after immunization of a single llama with VWF. The sdAb KB-V13 (formerly KB-VWF-013) has been previously characterized.[10] The anti-albumin nanobody KB-OptiAlb12 is a llama-derived nanobody that displays high-affinity binding (<5 nM) to both human and murine albumin. The chemically synthesised KB-V13A12 sequence was cloned into a pHEN6-plasmid, expressed in competent E.coli WK6 bacteria and purified by affinity chromatography using a HiTrap TALON column (GE Healthcare, Buc dans les Yvelines, France). A control bispecific sdAb (KB-V13AT02) was synthetized by cloning the KB-V13 linked to the previously described KB-AT02 against antithrombin.[11]

Purified bispecific sdAbs were administered subcutaneously (5mg/kg body weight) to isoflurane anesthetized mice. Blood was collected at the indicated time points for VWF antigen quantification

and multimer analysis. A separate group of mice was treated with KB-V13A12 and haemostasis was assessed 3 days post injection in a tail-clip assay, generally by a person blind to the treatment.

Tail-vein-transection model and tail-artery-transection model

In the tail-vein-transection (TVT) assay, an incision is applied to only one lateral tail vein. TVT was conducted as described[12] and consisted in a standardized 0.7 mm deep wound obtained sliding the blade of a scalpel through the transection groove of a customized metal template. Mice were anesthetized with isofluorane and warmed on a heating pad throughout the experimental procedure. If mice were not actively bleeding at 15-, 30- and 45-minute post-injury, the wound was challenged by gently wiping it twice in the distal direction. Blood shed by the wound after the injury was collected in isotonic saline solution (0.9% NaCl) for 60 minutes and quantified measuring haemoglobin optical density at 416 nm after red blood cell lysis.

Every spontaneous arrest of the bleeding was recorded. Bleeding profiles indicate bleeding (filled bars) and non-bleeding (empty bars) time periods throughout the 60-minute observation time.

The tail-artery-transection (TAT) model consists of a modified TVT model in which the ventral tail artery was transected using the same customized templates. Experimental time was set at 30 minutes.

Tail-clip model

A classic tail-clip assay was performed essentially as described.[13,14] Briefly, 3 mm of the distal tip of the tail of anesthetized mice (ketamine and xylazine, 100 and 10mg/kg, respectively) was amputated using a razor blade. Blood shed by the injury was collected in isotonic saline solution constantly warmed at 37°C for 30 min and quantified measuring haemoglobin optical density.

Histamine (Merck, Fontenay Sous Bois, France) was administered intraperitoneally (13 μmol/kg body weight)[15] 30 minutes prior to tail-clip or blood collection. The 30-minute time point was selected based on preliminary experiments showing that highest VWF levels were observed 30 minutes post-histamine administration (not shown).

Recombinant human VWF containing intact-VWF only (r-hVWF, Veyvondi, Takeda) was administered intravenously (50U/Kg body weight) 5 minutes before tail-clip or blood collection.

Saphenous vein puncture model

The saphenous vein puncture model was conducted essentially as described[16,17] on mice anesthetized with ketamine/xylazine (ketamine and xylazine, 100 and 10mg/kg, respectively) and constantly warmed on a heating pad. Briefly, a large saphenous vein was exposed and pierced with a 23G needle at equal distance between the femoral vein and the distal branches. The first clot was then gently

removed by wiping and a longitudinal incision of ~1mm was made on the exposed side of the vessel using micro-scissors. The blood leaking from the incision was gently absorbed until haemostasis occurred and blood clots were removed using a gauze swab humidified with 0.9 % NaCl. The number of clots formed during 30 minutes from the first incision was recorded.

In vivo ferric chloride-induced thrombus formation

Mice were anesthetized with ketamine/xylazine and the left carotid artery exposed. Thrombus formation was chemically initiated by applying for 2 minutes a filter paper (0.5x3mm) previously soaked in a freshly prepared $FeCl_3$ solution (15%). Blood flow was measured shortly before and after the $FeCl_3$-induced damage by using a Transonic console with perivascular flowmeter module equipped with a nanoprobe for transit-time ultrasound flow measurement (T402 console, TS420 flowmeter, MA0.5PSB probe, Transonic Europe, Elsloo, The Netherlands)[18]. Data were digitally acquired with a PowerLab 2/26 device and a LabChart 8.0 software (ADInstruments, Oxford, UK). Measurements were stopped 10-minutes post-occlusion, indicated by blood flow < 0.2ml/min for at least 10-consecutive minutes; or at 60 minutes in mice that did not occlude.

Platelet αIIbβ3 activation, α-granule release and surface receptor expression

Platelet αIIbβ3 activation and α-granule release studies were conducted in whole blood as previously described.[18,19]

Murine and human GPIbα expression was studied in murine platelets by flow cytometry as previously described[19]. Briefly, whole blood was incubated with an anti-murine GPIX-FITC antibody (clone Xia.B4, Emfret Analytics, Eibelstadt, Germany), an anti-murine GPIbα-PE (clone Xia.G5, Emfret) and an anti-human GPIbα-APC (clone HIP1, BD Biosciences, France).

Mouse platelet lysates

Platelet lysates were prepared as described[19] in the absence of platelet-activators.

Statistical analysis

All data are presented as mean±standard deviation (mean±SD). Number (n) refer to the number of animals. The statistical analysis was performed using GraphPad Prism 10 software for Mac (La Jolla, California, USA). One-way analysis of variance (1-way ANOVA) followed by Tukey's or Dunnett's multiple comparison test was performed when comparing multiple groups. Pairwise analysis was performed using the unpaired two-tailed Student's t-test. Two-way analysis was performed for two factors comparisons. $P<0.05$ was considered as statistically significant.

Table S1. Genotyping primers

			PCR product size (bp)	
		Sequence 5'-3'	**Wild-type allele**	**Knock-in allele**
VWF	**P1(common)**	CAAGTCTAACACAGATGGAGCACAGGTGAGT	**P1-P2 218**	**P1-P3 288 (+ 9370)**
	P2	GGACGGTGAGAACCAGCTCATTTCCT		
	P3	CTTGGCACTGTCCTCTCATGCGTTG		
GP1BA	**P4**	ACTCAAACCCAACAGGCTGCCAC	**P4-P5 226**	**P4-P5 305**
	P5	GCAGGTAGGACACCTCCACCTTAGTGA		

Figure S1

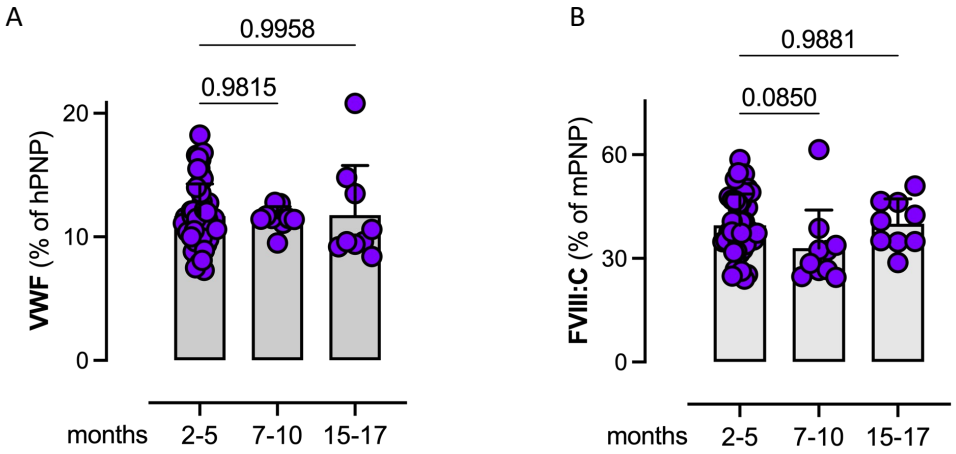

Supplemental Figure S1. VWF and FVIII levels over time

Panel A. VWF antigen levels and **Panel B.** FVIII activity levels in hVWD1 mice over a 15/17-month experimental time period. Data at 2/5 months as in Figure 1A and B.

A-B. Grey bars indicate mean±SD. Statistical analysis: One-way ANOVA with Dunnett correction for multiple comparisons.

Figure S2

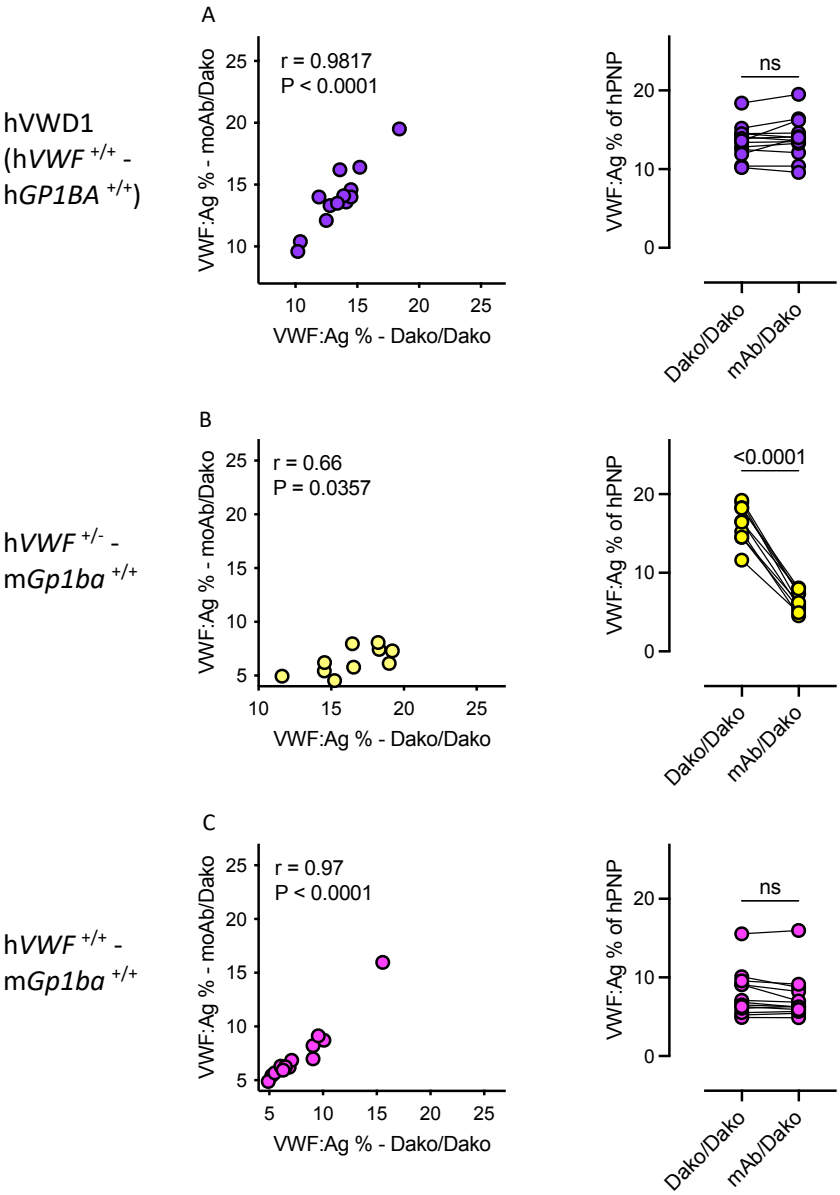

Supplemental Figure S2. VWF expression

VWF antigen levels were measured by two assays. One used commercial polyclonal antibodies that detected both human and murine VWF (Dako/Dako) and the second used a pool of monoclonal antibodies as coating-antibody, therefore detecting only human VWF (moAb/Dako). Both assays used the same detecting antibody and the same human-pooled plasma as reference. To evaluate if human or human & murine VWF was expressed in engineered mice, we evaluated the correlation between plasmatic VWF antigen levels measured by the two assays (graphs on the left) and directly compared raw values obtained for the same mouse in the two assays (graphs on the right). Data were measured for hVWD1 mice, homozygous for hVWF and hGPIbα (h*VWF* $^{+/+}$/h*GP1BA*$^{+/+}$) (**A**, n=13, purple), mice heterozygous for human-murine VWF and homozygous for mGPIbα (h*VWF* $^{+/-}$/m*Gp1ba*$^{+/+}$) (**B**, n=10,

light yellow) and mice homozygous for human VWF and murine GPIbα (h*VWF* $^{+/+}$/m*Gp1ba* $^{+/+}$) (**C**, n=13, pink).

An almost perfect correlation between values obtained in the two assays was observed in mice homozygous for h*VWF* expression (h*VWF* $^{+/+}$, A purple and C pink) irrespective of GPIbα expression (human in A and murine in C). These correlations corresponded to almost identical raw values in the two antigen assays (graphs on the right), supporting the notion that these mice only express human VWF, and that engineering GPIbα has no effects on VWF expression levels.

Despite a positive correlation was still measured for VWF antigen levels measured by the two assays in plasma from heterozygous mice for VWF (B, light yellow), raw antigen levels measured in the Dako/Dako assay were roughly twice as high as those measured in the moAb/Dako assay (right), supporting the notion that heterozygous mice for VWF express both human and murine VWF.

Altogether, these data are consistent with the hypothesis that hVWD1 mice only express hVWF.

Figure S3

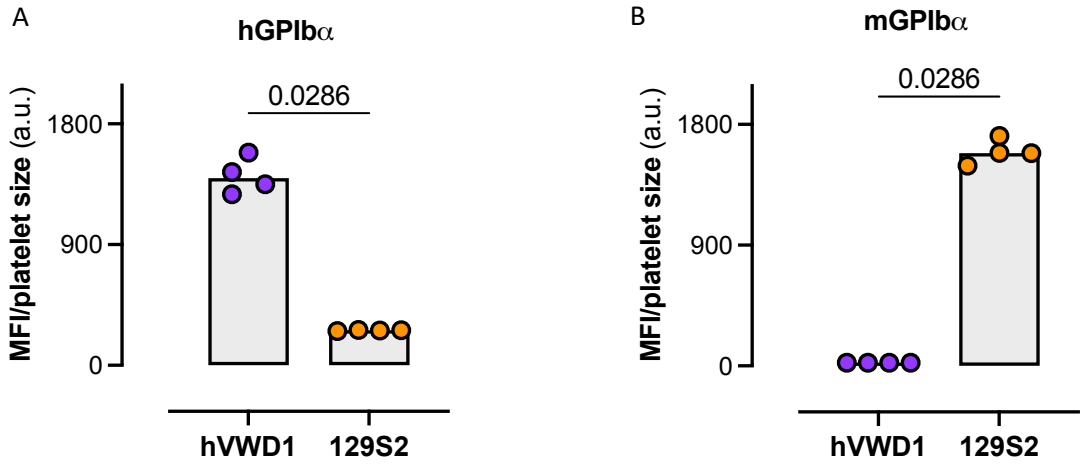

Supplemental Figure S3. Platelet surface expression of human or murine GPIbα

Platelet surface expression of human (**panel A**) or murine (**panel B**) GPIbα was confirmed by flow cytometry in hVWD1 (n=4, purple) and 129S2 (n=4, yellow) mice using specie-specific antibodies recognizing the human (anti-human GPIbα-APC) or murine (anti-murine GPIbα-PE) receptors. Histograms refer to the mean fluorescence intensity for APC (A) or PE (B) signals normalized by platelet size as measured by a veterinary counter. Platelets circulating in hVWD1 mice express human- but not murine GPIbα (purple). On the contrary, platelets circulating in 129S2 mice express murine- but not human GPIbα (yellow).

A-B Grey bars indicate mean±SD. Statistical analysis: Mann-Whitney test. Data of one representative experiment out of two, 4-8 mice per experiment. MFI: mean fluorescent intensity, a.u.: arbitrary units.

Figure S4

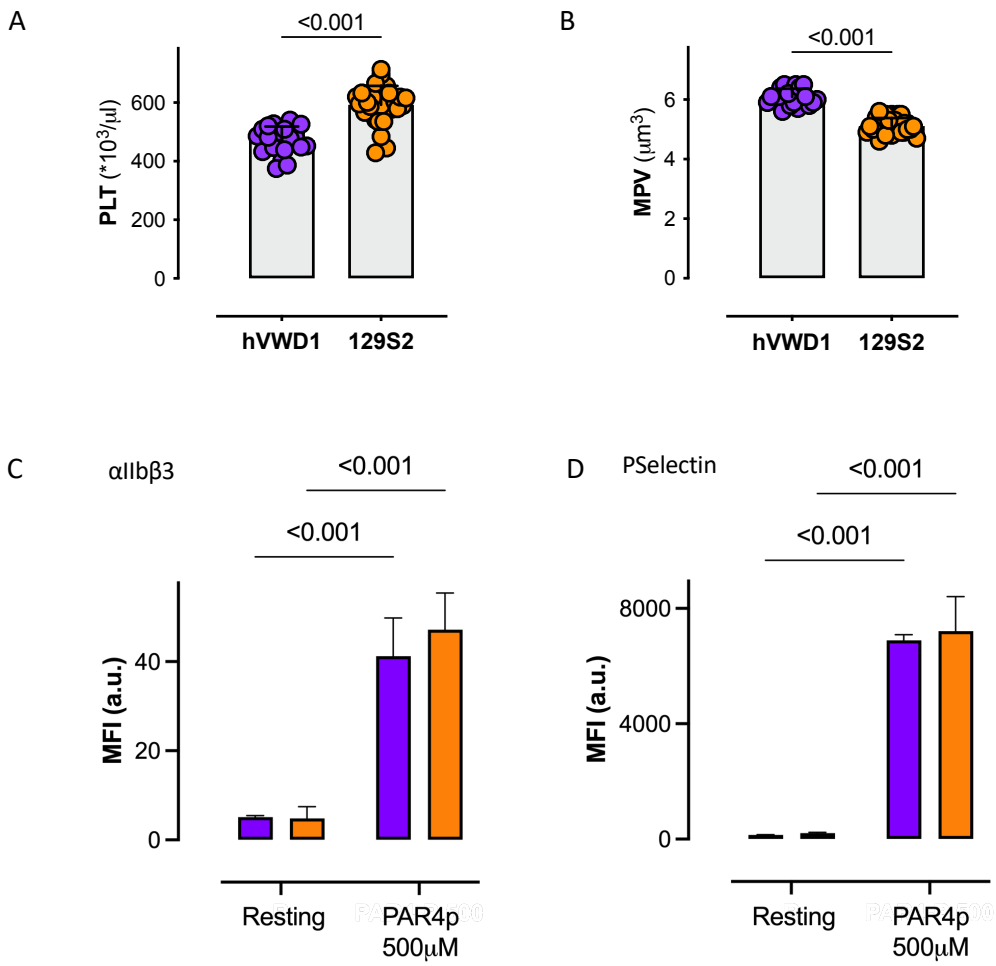

Supplemental Figure S4. Platelet studies in hVWD1 mice

Panel A. Peripheral platelet counts and **panel B.** mean platelet volume in hVWD1 (n=21, purple) and control (n=28, yellow) mice assessed in whole blood collected in 10% vol/vol EDTA 50 mM using an automatic cell counter (Scil Vet ABC Plus, Horiba Medical, France).

Panels C-D. Whole blood platelet activation. αIIbβ3 integrin activation (C) measured with JON/A-PE (Emfret Analytics, Germany) and (D) P-selectin surface expression (Rat anti-Mouse CD62p/AF647, Emfret Analytics, Germany) in resting and activated platelets (PAR4p 500µM, Bubendorf, Switzerland) from hVWD1- (n=4, purple) and control- (n=9, yellow) mice.

A-B Grey bars indicate mean±SD. Statistical analysis: A-B. two-tailed Student's t-test. C-D. two-way ANOVA with Sidak correction for multiple comparisons.

PLT: platelets, MPV: mean platelet volume, MFI: mean fluorescent intensity, a.u.: arbitrary units.

Figure S5

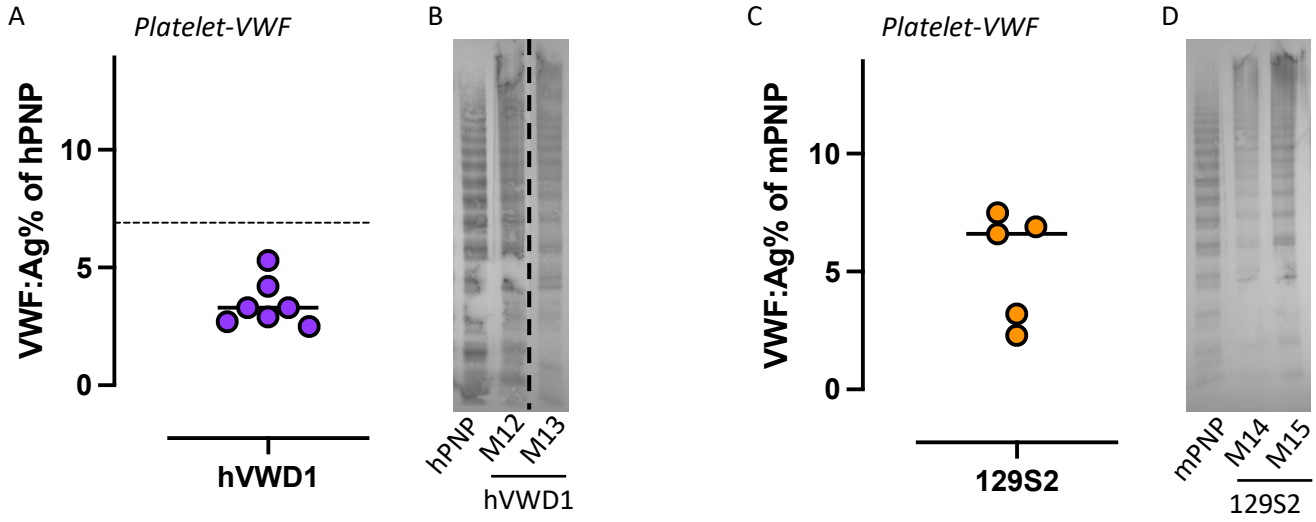

Supplemental Figure S5. Platelet VWF

Platelets were isolated from hVWD1- (purple) and 129S2-mice (yellow), washed and lysed as previously described[19]. **Panel A.** The amount of VWF in platelets from hVWD1 mice was quantified by ELISA using a human pooled normal plasma (hPNP) as reference. The values indicated in the graph refer to 10^8 platelets. The dotted line indicates VWF:Ag in 10^8 human platelets (internal data), which is consistent with data from the literature[20]. Importantly, for a direct comparison between murine hVWD1-platelets and human platelets, the difference in size and possibly in α-granules content should be taken into account, but was out of the scope of the present study. **Panel B.** Multimer profile of platelet-VWF in hVWD1 mice. As expected, platelets are enriched in HMWMs. Multimers were studied in 1.5% agarose gel by loading similar amount of VWF (≈10ng) in the hPNP, used as reference, and in two platelet lysate samples (from two individual mice, M12 and M13). The dotted line indicates non-consecutive lanes on the same gel. **Panel C.** The amount of VWF in platelets from 129S2 mice was quantified by ELISA using a murine pooled normal plasma (mPNP) as reference. The values indicated in the graph refer to 10^8 platelets. **Panel D.** Multimer profile of platelet-VWF in 129S2 mice. Multimers were performed as in B.

hPNP, human pooled normal plasma; mPNP, murine pooled normal plasma

Figure S6

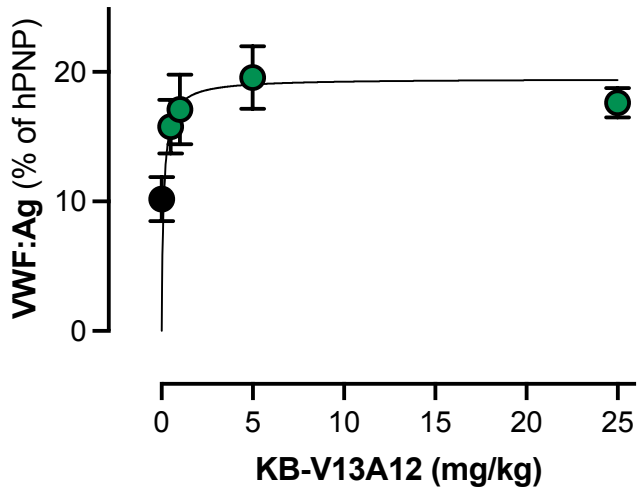

Comparisons	p value
0 vs 0.5 mg/kg	0.0002
0 vs 1 mg/kg	<0.0001
0 vs 5 mg/kg	<0.0001
0 vs 25 mg/kg	<0.0001
5 vs 0.5 mg/kg	0.0189
5 vs 1 mg/kg	0.1685
5 vs 25 mg/kg	0.2547

Supplemental Figure S6. Dose-response assessment of KB-V13A12

VWF:Ag was assessed in hVWD1 mice before (black) and 3 days post-sc administration of various doses (0.5, 1, 5, and 25 mg/kg) of KB-V13A12 (green).

Statistical analysis: One-way ANOVA with Holm-Sidak correction for multiple comparisons.

Supplementary References:

1. Banno F, Kaminaka K, Soejima K, Kokame K, Miyata T. Identification of Strain-specific Variants of Mouse Adamts13 Gene Encoding von Willebrand Factor-cleaving Protease. Journal of Biological Chemistry 2004;279(29):30896–30903.

2. Zhou W, Bouhassira EE, Tsai H-M. An IAP retrotransposon in the mouse ADAMTS13 gene creates ADAMTS13 variant proteins that are less effective in cleaving von Willebrand factor multimers. Blood 2007;110(3):886–893.

3. Flood VH, Johnsen JM, Kochelek C, et al. Common VWF sequence variants associated with higher VWF and FVIII are less frequent in subjects diagnosed with type 1 VWD. Res Pract Thromb Haemost 2018;2(2):390–398.

4. Johnsen JM, Auer PL, Morrison AC, et al. Common and rare von Willebrand factor (VWF) coding variants, VWF levels, and factor VIII levels in African Americans: the NHLBI Exome Sequencing Project. Blood 2013;122(4):590–597.

5. Mufti AH, Ogiwara K, Swystun LL, et al. The common VWF single nucleotide variants c.2365A>G and c.2385T>C modify VWF biosynthesis and clearance. Blood Adv 2018;2(13):1585–1594.

6. Lenting PJ, Westein E, Terraube V, et al. An experimental model to study the in vivo survival of von Willebrand factor. Basic aspects and application to the R1205H mutation. J Biol Chem 2004;279(13):12102–12109.

7. Groot E, Fijnheer R, Sebastian SA, de Groot PG, Lenting PJ. The active conformation of von Willebrand factor in patients with thrombotic thrombocytopenic purpura in remission. J Thromb Haemost 2009;7(6):962–969.

8. Pruthi RK, Daniels TM, Heit JA, Chen D, Owen WG, Nichols WL. Plasma von Willebrand factor multimer quantitative analysis by in-gel immunostaining and infrared fluorescent imaging. Thromb Res 2010;126(6):543–549.

9. Aymé G, Adam F, Legendre P, et al. A Novel Single-Domain Antibody Against von Willebrand Factor A1 Domain Resolves Leukocyte Recruitment and Vascular Leakage During Inflammation—Brief Report. ATVB 2017;37(9):1736–1740.

10. Muczynski V, Casari C, Moreau F, et al. A factor VIII-nanobody fusion protein forming an ultrastable complex with VWF: effect on clearance and antibody formation. Blood 2018;132(11):1193–1197.

11. Barbon E, Ayme G, Mohamadi A, et al. Single-domain antibodies targeting antithrombin reduce bleeding in hemophilic mice with or without inhibitors. EMBO Mol Med 2020;12(4):e11298.

12. Johansen PB, Tranholm M, Haaning J, Knudsen T. Development of a tail vein transection bleeding model in fully anaesthetized haemophilia A mice - characterization of two novel FVIII molecules. Haemophilia 2016;22(4):625–631.

13. Rayes J, Hollestelle MJ, Legendre P, et al. Mutation and ADAMTS13-dependent modulation of disease severity in a mouse model for von Willebrand disease type 2B. Blood 2010;115(23):4870–4877.

14. Marx I, Lenting PJ, Adler T, Pendu R, Christophe OD, Denis CV. Correction of bleeding symptoms in von Willebrand factor-deficient mice by liver-expressed von Willebrand factor mutants. Arterioscler Thromb Vasc Biol 2008;28(3):419–424.

15. Zirka G, Robert P, Tilburg J, et al. Impaired adhesion of neutrophils expressing Slc44a2/HNA-3b to VWF protects against NETosis under venous shear rates. Blood 2021;137(16):2256–2266.

16. Buyue Y, Whinna HC, Sheehan JP. The heparin-binding exosite of factor IXa is a critical regulator of plasma thrombin generation and venous thrombosis. Blood 2008;112(8):3234–3241.

17. Verhenne S, McCluskey G, Maynadié H, et al. Fitusiran reduces bleeding in factor X-deficient mice. Blood 2024;144(2):227–236.

18. Paul DS, Casari C, Wu C, et al. Deletion of the Arp2/3 complex in megakaryocytes leads to microthrombocytopenia in mice. Blood Adv 2017;1(18):1398–1408.

19. Casari C, Paul DS, Susen S, et al. Protein kinase C signaling dysfunction in von Willebrand disease (p.V1316M) type 2B platelets. Blood Adv 2018;2(12):1417–1428.

20. Fressinaud E, Baruch D, Rothschild C, Baumgartner HR, Meyer D. Platelet von Willebrand factor: evidence for its involvement in platelet adhesion to collagen. Blood 1987;70(4):1214–1217.